VIA MEDICA

Original article

NOWOTWORY Journal of Oncology
2021, volume 71, number 5, 267–273
DOI: 10.5603/NJO.a2021.0047
© Polskie Towarzystwo Onkologiczne
ISSN 0029–540X, e-ISSN: 2300-2115
www.nowotwory.edu.pl

What new dose distribution statistics may be included in the optimization of dose distribution in radiotherapy for post-mastectomy patients

Piotr Mężeński, Paweł Kukołowicz

Maria Sklodowska-Curie National Research Institute of Oncology, Warsaw, Poland

Introduction. The main aim of this study was to evaluate the doses delivered to heart substructures and calculate normal tissue complication probability (NTCP) for the intensity modulation radiotherpy (IMRT) irradiated group of left-sided post-mastectomy patients.

Material and methods. In this retrospective study for 30 randomly chosen breast cancer patients, the mean dose, V_2, V_4, V_{10}, V_{20} and D2% in the heart substructures were evaluated.

Results. The mean heart dose was 12.3 Gy, the mean left anterior descending artery (LAD) dose was 28.5 Gy. The average value of long-term cardiac mortality was 0.17%, pericarditis 0.0%, left ventricle perfusion defects 24.5% and LAD toxicity 0.2%. In the literature, for the IMRT technique for left-sided mastectomy patients, the mean heart dose ranged from 8.7–14.0 Gy and the V_{20} 10.5–14%. Additional studies are needed to describe the cardiac toxicity.

Conclusions. It is necessary to contour cardiac substructures for reliable assessment of the dose distribution, although the mean heart dose is simplification for modern radiotherapy techniques.

Key words: heart, breast cancer, post-mastectomy, IMRT, NTCP

Introduction

Many large randomized trials have demonstrated that post-mastectomy irradiation is beneficial, at least for patients with high-risk disease [1, 2]. However, for women irradiated on the left side, the dose delivered to the heart increases the risk of ischemic heart disease [3]. Taylor and co-workers have shown, there are many factors that affect doses deposited in the heart. The most important being the individual anatomy of a patient and the irradiation technique [4]. For older techniques, such as the tangential pair technique, the dose distribution in the heart and its substructures may be well estimated with the maximum heart distance (MHD) [4].

According to Darby, the cumulative relative risk of a major coronary event increases linearly by approximately 7% for each increase of 1 Gy of the mean heart dose in the tangential field technique [3]. The cumulative risk of death from ischemic heart disease is higher in radiotherapy patients compared to non-radiotherapy patients [3]. Uwe Schneider suggested [5] that in the intensity modulation techniques (IMRT) or volumetric modulated arc therapy (VMAT) techniques, with large volumes of the heart receiving low doses the risk of major coronary events might not be linear as proposed by Darby [3].

Despite these enormous changes in technology and irradiation methods, optimization of dose distributions in the

How to cite:

Mężeński P, Kukołowicz P. ***What new dose distribution statistics may be included in the optimization of dose distribution in radiotherapy for post-mastectomy patients.*** *NOWOTWORY J Oncol* 2021; 71: 267–273.

This article is available in open access under Creative Common Attribution-Non-Commercial-No Derivatives 4.0 International (CC BY-NC-ND 4.0) license, allowing to download articles and share them with others as long as they credit the authors and the publisher, but without permission to change them in any way or use them commercially.

heart is still based on the same assumptions. The dose to the heart is most often evaluated with the mean dose to the organ at risk. The heart is a complicated organ composed of muscular tissue, blood vessels, valves, nerve tissue fibres. The risk of damage to various heart structures by dosage may require a different quantitative description. Therefore, the statistics like the mean heart dose might not be the best predictor of all types of complications. An exact description of the interplay between radiotherapy and chemotherapy in heart damage is required. This is especially true in breast cancer patients, where systematic treatment is associated with heart toxicity [6, 7]. For post-mastectomy patients, there is a limited literature base describing doses received by individual heart structures in dynamic radiotherapy techniques [8]. Most of the available articles analyse the technique of two tangential fields in a group of breast conserving therapy patients (BCT).

The main aim of this study was to evaluate the doses delivered to substructures of the heart for the IMRT irradiated group of left-sided post-mastectomy patients. The doses to heart substructures were described in terms of dosed distribution and the model based on normal tissue complication probability (NTCP).

Material and methods

Patients

In this retrospective study for 30 randomly chosen breast cancer patients, we analysed the doses delivered to the heart and its substructures. All of these patients, of a median age of 53 years (32–88), were after a left-sided mastectomy. From the group of 30 patients, 29 patients underwent a modified radical mastectomy (MRM) with axillary fossa extraction, 1 patient had a simple mastectomy with a sentinel lymph node biopsy. Chemotherapy was applied throughout the group of 30 patients, 13 patients received pre-surgical chemotherapy. Radiotherapy was applied after surgery and chemotherapy. Pathological tumour nodus metastases (pTNM) staging was made according to the VII edition of the International Union Against Cancer (UICC) [9].

CT scan and contouring

Patients were placed supine in the treatment position, with their arms raised above their head, immobilized with OncoPoRT board. Computed tomography (CT) scans for treatment planning were acquired during free breathing, with 1.5 mm slice thickness, using a Siemens CT scanner. Scans were acquired from the hyoid bone to the end of the thoracic vertebrae, with 10 mm tissue-equivalent bolus placed on the thoracic wall. Next, the target volumes and organs at risk were delineated on the CT scans. For planning, the clinical target volume (CTV) included chest wall (CTV_{chest}) and axillary, infra and supraclavicular nodal areas (CTV_{nodes}) being delineated. Planning target volume (PTV) was created by adding a 6 mm isotropic margin to CTV. Organs at risk included the heart, lungs, coronary arteries, defined as 6 mm margins of the heart anterior wall and the spinal canal.

For the purpose of a retrospective analysis of the doses absorbed to the heart, additional heart substructures were segmented based on Mary Feng Cardiac Atlas Heart [10]. The contoured heart substructures were: the pericardium defined as 2 mm sac, created as margin from internal and external of the heart surface, ascending aorta, aortic arch, descending aorta, superior vena cava (SVC), inferior vena cava (IVC), pulmonary artery, coronary arteries: left coronary artery (LCA), left anterior descending coronary artery (LAD), left circumflex artery (LCX) and right coronary artery (RCA), left atrium, right atrium, left ventricle, right ventricle (fig. 1). Contoured structures were approved by a radiation oncologist.

Treatment planning and dose evaluation

For each patient, the IMRT treatment plan was prepared in Eclipse version 15 (Varian) treatment planning system. The total dose was 45 Gy, delivered in 2.25 Gy fraction doses. Dose distribution was calculated with the Analytical Anisotropic Algorithm (AAA) version 15. From five to seven 6 MV coplanar photon fields were used arranged in a fan pattern. The dose was prescribed to the CTV ($CTV_{wall} + CTV_{nodes}$) mean dose. During plan preparation, the following dose-volume constraints were used: for the PTV D98% > 95%, D2% < 107%, for the heart the mean dose <16 Gy and $V_{20} < 14\%$, for the lungs the mean dose <12 Gy, $V_{20} < 14\%$ and $V_{30} < 9\%$.

Treatment plans were retrospectively analysed. In each heart substructure the mean dose, V_2, V_4, V_{10}, V_{20} and D2% were evaluated.

Calculation of the NTCP

To calculate the NTCP, the Lyman Kutcher Burman (LKB) model was used (equations 1–3) [11].

$$NTCP = \frac{1}{\sqrt{2\pi}} \int_{-\infty}^{t} e^{\frac{x^2}{2}} dx \quad (1)$$

$$t = \frac{D_{eff} - TD_{50}}{mTD_{50}} \quad (2)$$

$$D_{eff} = (\Sigma_i V_i D_i^{1/n})^n \quad (3)$$

where: D_{eff} is the dose that, if given uniformly to the entire volume, will lead to the same NTCP as the non-uniform dose distribution, TD_{50} is the uniform dose delivered to the entire organ that results in a 50% complication risk, m is a measure of the slope of the sigmoid curve, n is the volume effect parameter, and V_i is the fractional organ volume receiving a dose D_i.

End-point model parameters were taken from the literature. Long term cardiac mortality (TD_{50} = 52.3 Gy, n = 1, m = 0.28, α/β = 3 Gy) [10], pericarditis (TD_{50} = 50.6 Gy, n = 0.64, m = 0.13, α/β = 2.5 Gy) [11], left ventricle perfusions defect (TD_{50} = 29 Gy, n = 0.16 m = 0.41 α/β = 2.5 Gy) [12], LAD toxicity (TD_{50} = 48 Gy, n = 0.35, m = 0.10, α/β = 2.5 Gy) [13].

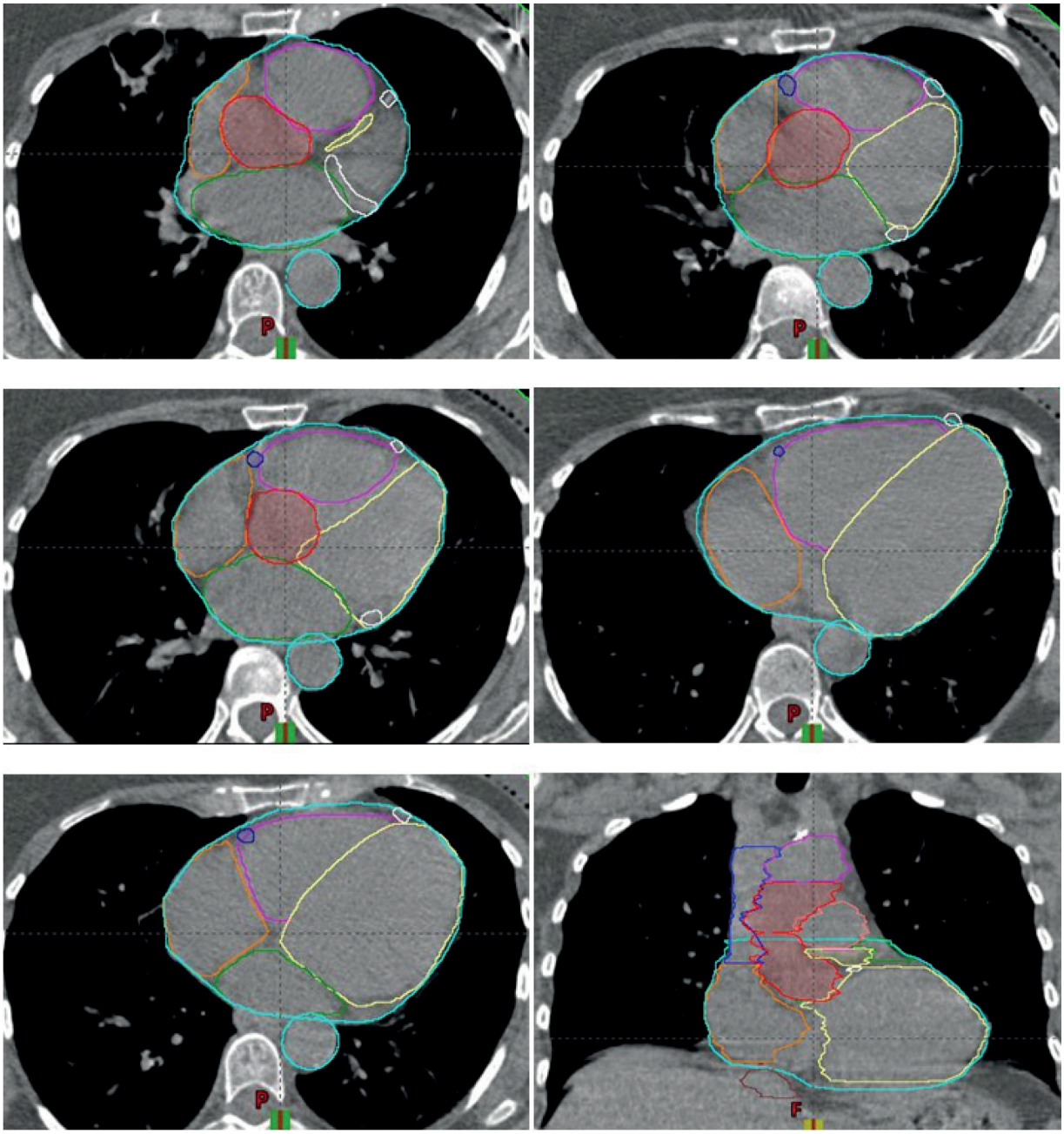

Figure 1. CT scan with heart substructures: cyan heart, red ascending aorta, magenta aortic arch, cyan descending aorta, blue superior vena cava, brown inferior vena cava, pink pulmonary artery, orange left atrium, green right atrium, yellow left ventricle, purple right ventricle, yellow LCA, white LAD, white LCX, blue RCA

Statistical Analysis

Data was described by the average value (AVG) and standard deviation (SD) of all analysed statistics obtained for the 30 patients – AVG (SD). For the relationship between dose distribution statistics and NTCP, dose fitted curves were done.

Results

Dose distribution in heart structures

Heart dose distribution parameters are summarised in table I. The average value of the mean heart dose was 12.3 Gy (1.1 Gy). The lowest average value of the mean dose was in IVC 5.5 Gy (1.4 Gy), the highest value of the mean dose was in LAD 28.5 Gy (5.0 Gy). The average value of V_{20} Gy in the heart was 11.5% (5.3%). The lowest average value of V_{20} Gy was in the descending aorta 0% (0%), IVC 0% (0%), SVC 0% (0%) and LCX 0% (0%). The highest average value of V_{20} Gy was in the LAD 73.3% (21.0%). The average value of the V_{10} in the heart was 59.9% (8.7%), the lowest average V_{10} value was in the vena cava inferior 0.2% (1.2%), the highest in the LAD 99.3% (3.4%). The average values of V_2–V_4 were high in all heart structures, 100% (0.2%) and 98.1%. The lowest value of V_2 and V_4 was in the descending aorta 87.1% (9.4%) and 72.6% (17.5%).

Table I. Average values and SD of dose distribution statistics in the group of 30 patients

	V_2 [%]	V_4 [%]	V_{10} [%]	V_{20} [%]	D m. [Gy]	D2% [Gy]
heart	100 (0.2)	98.1 (2.7)	52.9 (8.7)	11.5 (3.3)	12.3 (1.1)	33.8 (3.6)
pericardium	99.7 (1.1)	95.8 (5.3)	54.0 (7.6)	23.7 (6.1)	14.7 (1.7)	39.7 (3.3)
right ventricle	99.9 (0.3)	99.8 (1.3)	82.2 (13.3)	20.1 (9.5)	15.7 (2.3)	31.4 (5.5)
left ventricle	100 (0.1)	99.4 (1.6)	68.5 (17.5)	12.9 (5.6)	13.7 (1.7)	33.1 (5.1)
right atrium	99.9 (0.3)	96.2 (7.8)	19.9 (19.1)	0.1 (0.3)	7.9 (1.7)	13.8 (3.1)
left atrium	100 (0.0)	93.9 (11.7)	14.1 (15.3)	0.1 (0.1)	7.4 (1.6)	12.7 (2.6)
ascending aorta	100 (0.0)	99.9 (0.3)	49.5 (29.2)	3.7 (8.0)	10.8 (2.6)	17.8 (5.5)
aortic arch	100 (0.0)	100 (0.1)	70.5 (27.3)	11.0 (20.3)	13.4 (4.3)	21.1 (7.7)
descending aorta	87.1 (9.4)	72.6 (17.5)	5.3 (6.2)	0.0 (0.0)	5.5 (1.4)	10.7 (2.9)
SCV	100 (0.0)	98.5 (5.6)	16.8 (25.8)	0.0 (0.0)	8.0 (2.2)	10.7 (2.9)
IVC	100 (0.0)	85.8 (18.5)	0.2 (1.2)	0.0 (0.0)	5.7 (1.3)	7.3 (1.3)
pulmonary artery	100 (0.0)	99.4 (2.2)	65.9 (19.1)	12.1 (12.0)	13.1 (3.0)	25.6 (5.9)
LCA	100 (0.0)	100 (0.0)	65.9 (35.2)	0.6 (2.0)	11.7 (2.4)	14.8 (3.5)
LAD	100 (0.0)	100 (0.0)	99.3 (3.4)	73.3 (21.0)	28.5 (5.0)	40.3 (4.1)
LCX	100 (0.0)	98.4 (6.1)	45.3 (35.8)	0.0 (0.0)	9.7 (2.4)	12.5 (2.8)
RCA	100 (0.0)	100.0 (0.0)	73.8 (35.9)	6.3 (17.1)	12.9 (3.6)	15.8 (4.9)

VX – volume receiving X Gy and more; D m. – mean dose; D2% – near-maximum dose

NTCP values

Long term cardiac mortality

The average value of the long-term cardiac mortality for 30 patients was 0.17% (0.04%). Graphs present the NTCP-dose relationship for which the value of $R^2 > 0.5$. For the relationship between long-term cardiac mortality and the mean heart dose, the second degree polynomial was fitted ($R^2 = 0.96$), for V_{20} ($R^2 = 0.76$) and for V_{10} ($R^2 = 0.70$) a linear fit was used (fig. 2–4).

Pericarditis

In the group of 30 patients, the average value of the calculated NTCP for pericarditis was 0.0% (0.0%).

Left ventricle perfusions defect

The average value of left ventricle perfusion defects in 30 patients was 24.5% (8.0%). The graphs present the NTCP-dose relationship for which the value of $R^2 > 0.5$. For the relationship between left ventricle perfusion defects and D2%, the second-degree polynomial was fitted (R^2=0.97), for V20 ($R^2 = 0.68$) a linear fit was applied (fig. 5–6).

LAD toxicity

The average value of LAD toxicity in 30 patients was 0.2% (0.4%). The graphs presents the NTCP-dose relationship for which the value of $R^2 > 0.5$. For the relationship between LAD toxicity and the mean LAD dose (fig. 7), a two-parameter exponential function was fitted ($R^2 = 0.95$).

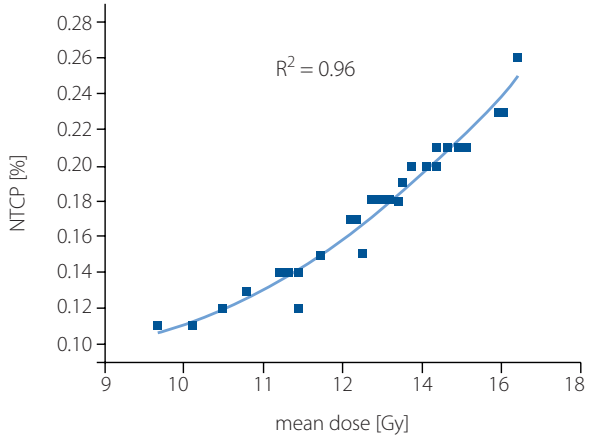

Figure 2. Relationship between the mean heart dose and long term cardiac mortality

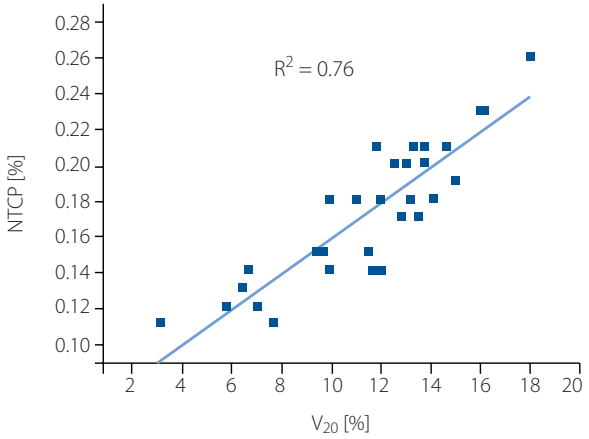

Figure 3. Relationship between heart V_{20} and long term cardiac mortality

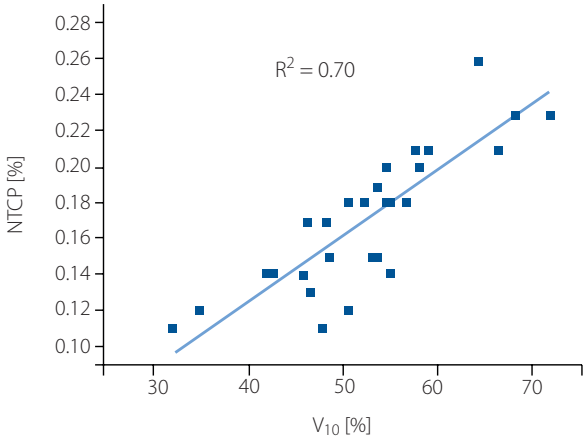

Figure 4. Relationship between heart V_{10} and long term cardiac mortality

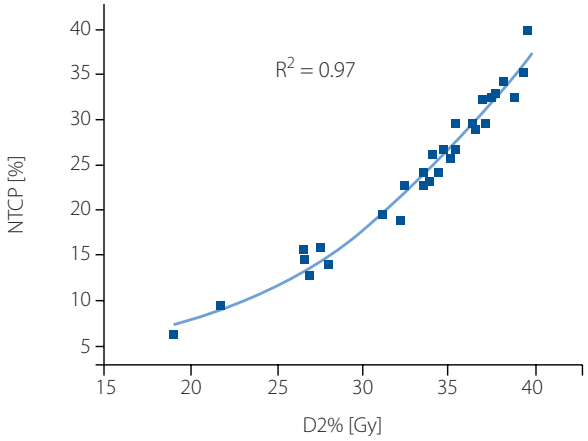

Figure 5. Relationship between D2% left ventricle dose and left ventricle perfusion defects

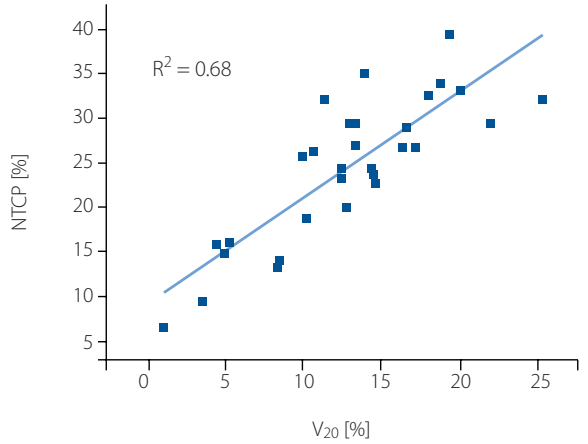

Figure 6. Relationship between V_{20} left ventricle dose and left ventricle perfusion defects

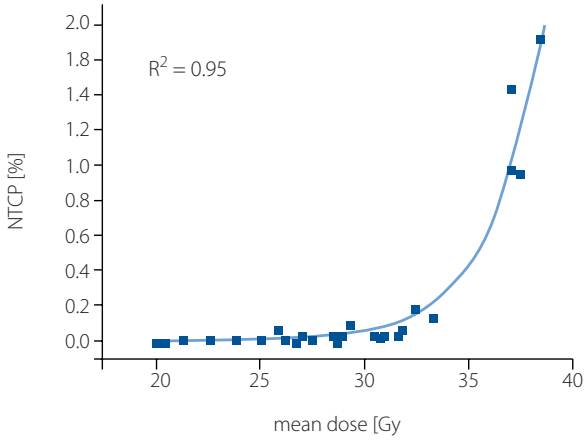

Figure 7. Relationship between mean LAD dose and LAD toxicity

Discussion

Dose distribution in heart structures

In our group of patients, the average value of the mean heart doses was 12.3 Gy (1.1 Gy) and the average volume V_{20} was 11.5% (3.3%). In the literature, for the IMRT technique for left-sided mastectomy patients, the mean heart dose ranged from 8.7 Gy to 14.0 Gy [12, 13] and the V_{20} value from 10.5% (5.2%) to 14% (6%)[12, 14, 15]. A large dispersion of the V_{10} also occurs in literature, a V_{10} ranged from 17.8% (7.1%) to 55.7% (29.6%) [12, 13, 15, 16].

Due to the proximity of the heart to PTV, the mean dose received by the left ventricle was 13.7 Gy (1.7 Gy) and 15.7 Gy (2.3 Gy) for the right ventricle. The D2% were 33.1 Gy (5.1 Gy) for the left ventricle and 31.4 Gy (5.5 Gy) for the right ventricle. In Li Zhang's article, a similar analysis was carried out for the IMRT technique and the mean left ventricle dose and the maximum left ventricle dose came to 12.7 Gy and 48.7 Gy, respectively, whereas the right ventricle mean dose was 14.7 Gy [8].

Among coronary arteries, the highest average values of mean dose of 28 Gy (5 Gy), was obtained for LAD. In Li Zang's article describing the IMRT technique for post-mastectomy patients, a high mean dose value of 37.7 Gy for LAD was obtained [8]. The high dose values received by LAD were also reported by other authors. In J. Caudrelier's article about the IMRT technique in BCT patients, a higher median dose and maximum doses for LAD of 10.8 Gy (7.8 Gy) and 26.7 Gy (15.7 Gy) and RCA of 12.4 Gy (5.7 Gy) and 27.0 Gy (12.4 Gy) were reported [17]. In our group of patients, the RCA average values of the mean dose were 12.9 Gy (3.6 Gy), and D2% – 15.8 Gy (4.9 Gy). In the LCA, average values of the mean dose were 11.7 Gy (2.4 Gy) and D2 – 14.8 Gy (3.5 Gy). The lowest values of the mean dose – 9.7 Gy (2.4 Gy), and D2% – 12.5 Gy (2.8 Gy) were obtained by the LCX similar to J. Caudrelier's article where the median dose was 4.5 Gy (1.7 Gy) and a maximum dose was 8.8 Gy (3.2 Gy) for LCX [17].

In the case of the IMRT technique, many therapeutic beams are used to achieve a conformal dose distribution. This results in an increased amount of scattered radiation which leads to an increase in the volume of tissues exposed to low doses. The dose range of 2–4 Gy covers from 100% to 72.6% of the volume of the heart structures.

NTCP values in IMRT

NTCP models take the form of empirical models based on dose distribution statistics from the treatment planning system and data from prospective and retrospective clinical trials. The values of the parameters used in radiobiological models are obtained by fitting curves to clinical data. The calculated NTCP value is always susceptible to the limitations of the used model and results from the uncertainty parameters used for modelling. The complicated structure of the heart causes that the probability of injuries of different heart structures is unlikely to be well described with a single parameter of dose distribution eg. mean dose [3].

Long term cardiac mortality

Darby estimated [3] the linear increase in the risk of major coronary events with a rising mean heart dose. This result was obtained for breast cancer patients irradiated with two tangential fields. In this technique, a small volume of the heart receives a high dose but the mean dose in the heart is smaller than in IMRT. Uwe Schneider suggested [5], that in IMRT, VMAT techniques there were large volumes of the heart receiving low doses the risk of major coronary events might not be linear as proposed by Darby [3]. The NTCP calculated by Schneider with Darby's data showed that the risk has a sigmoidal nature; it can be considered negligible if the mean heart dose does not exceed 15 Gy.

The probability of heart damage related with the mean heart dose analysed in this paper for IMRT for left-sided mastectomy patients showed similarity with Schneider's results. For a mean heart dose of 12 Gy, the LKB model based the probability of long term cardiac mortality at only 0.17%. A limitation of this approach is to use the same mean heart dose parameter to calculate NTCP for IMRT and the tangential field technique, due to different dose distributions in the heart.

Pericarditis

Pericarditis is the first clinical symptom for which dose-volume effect was found. In patients undergoing mediastinal radiotherapy, estimated pericarditis was about 6% if more than 50% of the external heart contour was in the radiation therapy field [18]. The probability of pericarditis was reduced from 20% to 7% by using left ventricle shielding and reduced to about 2.5% by shielding the left ventricle after 30 Gy [19]. Martel considered a mean dose of 27.1 Gy and a maximum dose of 47 Gy as predictors of pericarditis [20]. Wei and co-authors considered the volume of pericardium receiving a dose of 30 Gy and more (V_{30}) as statistics associated with the occurrence of complications [21]. The probability of pericarditis estimated by Wei was about 13%, if the $V_{30} < 46\%$ or a mean dose <26 Gy. If the mean dose exceeds 26 Gy and the V_{30} exceeds 46%, the probability increases to about 73% [21].

In the analysed group of 30 patients irradiated with IMRT, for a mean pericardial dose of 14.8 Gy and V_{20} of 23.7%, the LKB model based the probability of pericarditis at 0%.

Left ventricle perfusion defects

The clinical manifestation of subclinical perfusion defects is not well understood and the perfusion changes themselves can be reversible [22]. Based on single-photon emission computed tomography (SPECT) perfusion scans, Marks et al. demonstrated perfusion defects, limited to the part of the myocarcium which had received a dose higher than 15 Gy [22]. In the five-year follow-up, a reduction of the left ventricular wall contractility was demonstrated. The NTCP of left ventricular perfusion defects, estimated by Das et al. by LKB and relative seriality (RS) models, shows that this complication can be classified as for a serial organ [23]. Marks et al. analysed the left ventricular perfusion defects in a group of 73 breast cancer patients irradiated by the tangential fields technique [22]. The probability of damage was estimated to be below 20% if less than 5% of the left ventricle volume was in the therapeutic field. The probability of perfusion defects increases if more than 5% of the left ventricle volume is in the therapeutic field. Literature reports indicate a proportional increase in risk with an increase in the left ventricular volume and an increase in the mean left ventricle dose when the tangential field technique is used [24].

The average value of the LKB model based the probability of left ventricular perfusion in the group of 30 IMRT patients at 24.5% (8.0%) with a serial-like nature of the complication. An increase in the D2% in the left ventricle results in increasing NTCP .

LAD toxicity

Literature indicates the high sensitivity of coronary arteries to exposure from ionizing radiation. This is particularly important for the LAD, as an artery associated with the development of myocardial infarction in breast cancer patient radiotherapy [25]. The studies showed a higher percentage of LAD stenosis in patients undergoing left-sided radiotherapy for breast cancer, due to the presence of LAD in the therapeutic field and the large doses received by this artery [26–29]. The relationship between the occurrence of radiation damage and the coronary arteries indicated that the coronary arteries should be treated as a separate organ at risk, and tolerance doses may differ from the doses of tolerance for the remaining structures of the heart [30]. Some authors claim that high point doses in the coronary arteries can lead to an increased risk of myocardial infarction within 10 years from the application of radiotherapy [24].

The average LKB model based probability of LAD toxicity was 0.2% (0.4%). For the mean LAD dose and NTCP pseudo-threshold relationship was shown ($R^2 = 0.95$). Below 30 Gy of the mean LAD dose, the probability seems to be negligible. Pseudo-threshold may by caused by small group of patients, so can greatly impact the fit. Due to the small amount of data available and the difficulty in precise contouring, modelling LAD damage is challenging. Additional studies are needed to describe the LAD threshold doses and dose-volume relationships.

Conclusions

The collected data show that the assessment of the quality of the treatment plan for patients after a left-sided mastectomy performed only with the mean heart dose can be a significant simplification for modern radiotherapy techniques. It seems necessary to draw individual heart substructures for reliable assessment of the dose distribution and NTCP calculation.

Conflict of interest: none declared

Piotr Mężeński
Maria Sklodowska-Curie National Research Institute of Oncology
ul. Roentgena 5
02-781 Warszawa, Poland
e-mail: grandys@gmail.com

Received: 26 Mar 2021
Accepted: 1 Jul 2021

References

1. Kirova YM, Loap P, Fourquet A. Benefit of Post Mastectomy Radiation Therapy (PMRT) in Node-Positive, HER2-Positive Patients With Breast Cancer Receiving Anti-HER2 Treatments. Int J Radiat Oncol Biol Phys. 2020; 106(3): 511–513, doi: 10.1016/j.ijrobp.2019.12.022, indexed in Pubmed: 32014148.
2. McGale P, Taylor C, Correa C, et al. EBCTCG (Early Breast Cancer Trialists' Collaborative Group). Effect of radiotherapy after mastectomy and axillary surgery on 10-year recurrence and 20-year breast cancer mortality: meta-analysis of individual patient data for 8135 women in 22 randomised trials. Lancet. 2014; 383(9935): 2127–2135, doi: 10.1016/S0140-6736(14)60488-8, indexed in Pubmed: 24656685.
3. Darby SC, Ewertz M, McGale P, et al. Risk of ischemic heart disease in women after radiotherapy for breast cancer. N Engl J Med. 2013; 368(11): 987–998, doi: 10.1056/NEJMoa1209825, indexed in Pubmed: 23484825.
4. Kong FM, Klein EE, Bradley JD, et al. The impact of central lung distance, maximal heart distance, and radiation technique on the volumetric dose of the lung and heart for intact breast radiation. Int J Radiat Oncol Biol Phys. 2002; 54(3): 963–971, doi: 10.1016/s0360-3016(02)03741-0, indexed in Pubmed: 12377351.
5. Schneider U, Ernst M, Hartmann M. The dose-response relationship for cardiovascular disease is not necessarily linear. Radiat Oncol. 2017; 12(1): 74, doi: 10.1186/s13014-017-0811-2, indexed in Pubmed: 28449708.
6. Abouegylah M, Braunstein LZ, Alm El-Din MA, et al. Evaluation of radiation-induced cardiac toxicity in breast cancer patients treated with Trastuzumab-based chemotherapy. Breast Cancer Res Treat. 2019; 174(1): 179–185, doi: 10.1007/s10549-018-5053-y, indexed in Pubmed: 30478787.
7. Soumarová R, Rušinová L. Cardiotoxicity of breast cancer radiotherapy - overview of current results. Rep Pract Oncol Radiother. 2020; 25(2): 182–186, doi: 10.1016/j.rpor.2019.12.008, indexed in Pubmed: 32021574.
8. Zhang Li, Mei X, Chen X, et al. Estimating cardiac substructures exposure from diverse radiotherapy techniques in treating left-sided breast cancer. Medicine (Baltimore). 2015; 94(18): e847, doi: 10.1097/MD.0000000000000847, indexed in Pubmed: 25950697.
9. Ferretti S, Patriarca S, Carbone A, et al. [TNM classification of malignant tumours, VII edition 2009. Changes and practical effects on cancer epidemiology]. Epidemiol Prev. 2010; 34(3): 125–128, indexed in Pubmed: 20852350.
10. Feng M, Moran JM, Koelling T, et al. Development and validation of a heart atlas to study cardiac exposure to radiation following treatment for breast cancer. Int J Radiat Oncol Biol Phys. 2011; 79(1): 10–18, doi: 10.1016/j.ijrobp.2009.10.058, indexed in Pubmed: 20421148.
11. Deasy J. Comments on the use of the Lyman-Kutcher-Burman model to describe tissue response to nonuniform irradiation (multiple letters). Int J Radiat Oncol Biol Phys. 2000; 47(5): 1458–1459, doi: 10.1016/s0360-3016(00)00500-9.
12. Ma J, Li J, Xie J, et al. Post mastectomy linac IMRT irradiation of chest wall and regional nodes: dosimetry data and acute toxicities. Radiat Oncol. 2013; 8: 81, doi: 10.1186/1748-717X-8-81, indexed in Pubmed: 23566488.
13. Ma C, Zhang W, Lu J, et al. Dosimetric Comparison and Evaluation of Three Radiotherapy Techniques for Use after Modified Radical Mastectomy for Locally Advanced Left-sided Breast Cancer. Sci Rep. 2015; 5: 12274, doi: 10.1038/srep12274, indexed in Pubmed: 26194593.
14. Ma C, Zhang W, Lu J, et al. Dosimetric Comparison and Evaluation of Three Radiotherapy Techniques for Use after Modified Radical Mastectomy for Locally Advanced Left-sided Breast Cancer. Sci Rep. 2015; 5: 12274, doi: 10.1038/srep12274, indexed in Pubmed: 26194593.
15. Li W, Ma J, Chen J, et al. IMRT Versus 3D-CRT for Postmastectomy Irradiation of Chest Wall and Regional Nodes: A Population-Based Comparison of Normal Lung Dose. Int J Clin Exp Med. 2014; 90(1): S246–S247, doi: 10.1016/j.ijrobp.2014.05.869.
16. Landis DM, Luo W, Song J, et al. Variability among breast radiation oncologists in delineation of the postsurgical lumpectomy cavity. Int J Radiat Oncol Biol Phys. 2007; 67(5): 1299–1308, doi: 10.1016/j.ijrobp.2006.11.026, indexed in Pubmed: 17275202.
17. Caudrelier JM, Meng J, Esche B, et al. IMRT sparing of normal tissues in locoregional treatment of breast cancer. Radiat Oncol. 2014; 9: 161, doi: 10.1186/1748-717X-9-161, indexed in Pubmed: 25052720.
18. Gagliardi G, Constine LS, Moiseenko V, et al. Radiation dose-volume effects in the heart. Int J Radiat Oncol Biol Phys. 2010; 76(3 Suppl): S77–S85, doi: 10.1016/j.ijrobp.2009.04.093, indexed in Pubmed: 20171522.
19. Carmel R, Kaplan H. Mantle irradiation in Hodgkin's disease.An analysis of technique, tumor eradication, and complications. Cancer. 1976; 37(6): 2813–2825, doi: 10.1002/1097-0142(197606)37:6<2813::aid-cncr2820370637>3.0.co;2-s.
20. Ph.D. MM, M.D. WS, Ph.D. RT, et al. Fraction Size and Dose Parameters Related to the Incidence of Pericardial Effusions. Int J Radiat Oncol Biol Phys. 1998; 40(1): 155–161, doi: 10.1016/s0360-3016(97)00584-1.
21. Wei X, Liu HH, Tucker SL, et al. Risk factors for pericardial effusion in inoperable esophageal cancer patients treated with definitive chemoradiation therapy. Int J Radiat Oncol Biol Phys. 2008; 70(3): 707–714, doi: 10.1016/j.ijrobp.2007.10.056, indexed in Pubmed: 18191334.
22. Marks LB, Yu X, Prosnitz RG, et al. The incidence and functional consequences of RT-associated cardiac perfusion defects. Int J Radiat Oncol Biol Phys. 2005; 63(1): 214–223, doi: 10.1016/j.ijrobp.2005.01.029, indexed in Pubmed: 16111592.
23. Das SK, Baydush AH, Zhou S, et al. Predicting radiotherapy-induced cardiac perfusion defects. Med Phys. 2005; 32(1): 19–27, doi: 10.1118/1.1823571, indexed in Pubmed: 15719950.
24. Trott KR, Doerr W, Facoetti A, et al. Biological mechanisms of normal tissue damage: importance for the design of NTCP models. Radiother Oncol. 2012; 105(1): 79–85, doi: 10.1016/j.radonc.2012.05.008, indexed in Pubmed: 22748390.
25. Schultz-Hector S, Trott KR. Radiation-induced cardiovascular diseases: is the epidemiologic evidence compatible with the radiobiologic data? Int J Radiat Oncol Biol Phys. 2007; 67(1): 10–18, doi: 10.1016/j.ijrobp.2006.08.071, indexed in Pubmed: 17189062.
26. Correa CR, Litt HI, Hwang WT, et al. Coronary artery findings after left-sided compared with right-sided radiation treatment for early-stage breast cancer. J Clin Oncol. 2007; 25(21): 3031–3037, doi: 10.1200/JCO.2006.08.6595, indexed in Pubmed: 17634481.
27. Nilsson G, Holmberg L, Garmo H, et al. Distribution of coronary artery stenosis after radiation for breast cancer. J Clin Oncol. 2012; 30(4): 380–386, doi: 10.1200/JCO.2011.34.5900, indexed in Pubmed: 22203772.
28. Taylor CW, Nisbet A, McGale P, et al. Cardiac exposures in breast cancer radiotherapy: 1950s-1990s. Int J Radiat Oncol Biol Phys. 2007; 69(5): 1484–1495, doi: 10.1016/j.ijrobp.2007.05.034, indexed in Pubmed: 18035211.
29. Taylor CW, Povall JM, McGale P, et al. Cardiac dose from tangential breast cancer radiotherapy in the year 2006. Int J Radiat Oncol Biol Phys. 2008; 72(2): 501–507, doi: 10.1016/j.ijrobp.2007.12.058, indexed in Pubmed: 18374500.
30. Bruzzaniti V, Abate A, Pinnarò P, et al. Dosimetric and clinical advantages of deep inspiration breath-hold (DIBH) during radiotherapy of breast cancer. J Exp Clin Cancer Res. 2013; 32: 88, doi: 10.1186/1756-9966-32-88, indexed in Pubmed: 24423396.